Journal of Applied Polymer Science

Aqueous PUA emulsion prepared by dispersing polyurethane prepolymer in polyacrylate emulsion

Caideng Yuan, Jingpeng Wang, Mingtong Cui, Yan Peng
Department of Polymer Science and Engineering, School of Chemical Engineering and Technology, Tianjin University, Tianjin 300072, China
Correspondence to: C. Yuan (E-mail: cdyuan@tju.edu.cn)

ABSTRACT: Waterborne polyurethane/polyacrylate (PUA) emulsions were prepared by dispersing polyurethane (PU) prepolymer in polyacrylate (PA) emulsion; therefore, the PU particles formed in the presence of PA nanoparticles. The particle size and its distribution of the composite PUA emulsion were determined by dynamic light scattering. The result shows that the average particle size increases initially and then decreases with increasing PA content, which is confirmed by transmission electron microscope characterization. The surface properties of PUA films were analyzed by water contact angle and atomic force microscope topography. It indicates that the water contact angle and the average roughness of the composite PUA films are larger than those of the PU film. Meanwhile, mechanical properties test, scanning electron microscopy, and thermogravimetric analyses disclose that the PUA films are characterized by enhanced tensile strength, rough fractured surface, and good thermal stability. The preparation method proposed in this article is an effective and convenient way to manufacture composite PUA emulsion. The composite PUA emulsion can be potentially used in coatings. © 2015 Wiley Periodicals, Inc. J. Appl. Polym. Sci. **2016**, *133*, 43203.

KEYWORDS: blends; coatings; emulsion polymerization; polyurethanes; properties and characterization

Received 8 September 2015; accepted 10 November 2015
DOI: 10.1002/app.43203

INTRODUCTION

Polyurethane (PU) has been extensively used for coatings, adhesives, foams, biomimetic materials, and other applications due to its excellent flexibility, high ductility, strong adhesion, and good abrasion resistance.[1–5] In the past decades, solvent-based polymers, including PU, have been widely applied in varieties of fields followed by serious environmental problems. Nowadays, waterborne polyurethane (WPU), which is environment-friendly, has been attracting much attention both theoretically and practically from researchers all over the world.[6,7] WPU has significantly replaced solvent-based systems[8]; however, its use is seriously limited because of low stiffness and weak water resistance. To overcome such limitations of WPU, it is a common practice to incorporate other substances into WPU by copolymerization or hybrid emulsion polymerization.[9,10] In terms of PUAs, PUAs have a wide range of applications such as painting, coatings, adhesives, foams, textiles, membranes, packaging overcoat films, and biomedical materials, especially for oligomers. The wide application originates from its unique properties, including high solution, low melting viscosity, and three-dimensional architectures.[11–13] On one hand, UV-curable polyurethane acrylate (PUA) represents a major trend due to concern about environmental impacts and low energy consumption; however, one major drawback is their polymerization shrinkage, which would lead to failure and shorten service life of photopolymerization materials.[14] On the other hand, waterborne polyurethane polyacrylate (PUA) is an important class of materials, especially in the painting and coating in industry. The kind of PUA can be formed by mixing PU and PA emulsion or radical copolymerization.[15,16] Park *et al.*[17] prepared waterborne polyurethane/self-cross-linkable fluorinated acrylic emulsion by hybrid emulsion polymerization. Shin *et al.*[18] fabricated waterborne fluorinated polyurethane-acrylate copolymer by copolymerization. Xu *et al.*[19] first synthesized vinyl-terminated waterborne polyurethane-acrylate prepolymer and polyurethane/polyacrylate (PUA) copolymer was obtained by UV-curing technology. Although those ways result in the development of permanent covalent linkages between PU and acrylate, the process is usually complicated and gel is easy to be formed in the polymerization process.

Recently, physical mixing technology has been becoming popular, which is a quite versatile technique. Through this technology, diverse composite materials have already been synthesized.[20–22] Waterborne acrylic polymers have been paid more and more attention because of excellent resistance to hydrolysis and low cost.[23] The combination of PU dispersion

Table I. Formula of PA Emulsion, PU Prepolymer, and PUA Emulsion

PA emulsion		PU prepolymer		PUA emulsion	
Reagent	Mass ratio (%)	Reagent	Mass ratio (%)	Sample no.	PA to PU
DW	81.14	IPDI	38.47	PUA-0	0.0/10.0
MMA	14.80	DL-400	4.25	PUA-5	0.5/9.5
BA	2.61	DL-2000	43.03	PUA-10	1.0/9.0
HEMA	0.87	DMPA	5.04	PUA-15	1.5/8.5
AA	0.17	MN-400	9.20	PUA-20	2.0/8.0
SDS	0.26	DBTDL	(trace)	PUA-25	2.5/7.5
APS	0.14			PUA-30	3.0/7.0
				PUA-35	3.5/6.5
				PUA-40	4.0/6.0

and polyacrylate (PA) emulsion to achieve the best properties is attractive in many application fields.[24] Brown *et al.*[25] obtained PUA blends by mixing PA emulsions and commercial PU dispersions. The result showed that the tensile strength of the PUA blend films became lower than that of the PU film. Shu *et al.*[26] got PU and PA blend latex using the same method. The tensile strength was 8.8 and 5.6 MPa for films from core–shell PUA composite latex and PU + PA blend latex, respectively, showing that the core–shell PUA composite latex had better mechanical properties than their corresponding physical blend latex.

Compared to the physical mixing of PU dispersion and PA emulsion, dispersing PU prepolymer in PA emulsion, it will be helpful to enhance the properties of the composite materials and simplify the manufacturing process. The PU particles can be formed in the presence of PA nanoparticles, rather than by simple physical mixing. In this article, the PUA emulsion was prepared by dispersing PU prepolymer in PA emulsion. The particle size distribution and morphologies were characterized by dynamic light scattering (DLS) and transmission electron microscopy (TEM). The film properties were also detected and studied with water contact angle and atomic force microscope (AFM). The mechanical performance of the composite materials was measured and discussed. The results show that the PUA particle prepared by dispersing PU prepolymer in PA emulsion is with core–shell structure and exhibits relatively high performance.

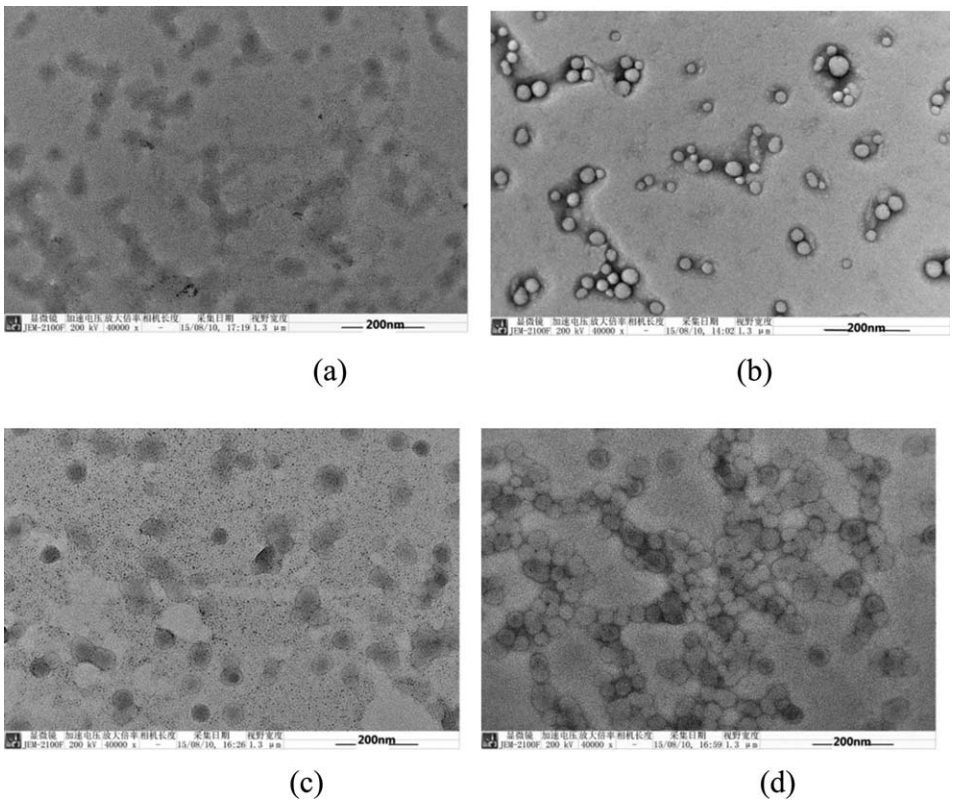

Figure 1. TEM micrographs of (a) PUA-0, (b) PA, (c) PUA-20, and (d) PUA-30 emulsion particles.

Table II. Properties of PUA Emulsions

Sample no.	Particle size (nm)	PSD index	Storage stability
PUA-0	70	0.142	Stable
PUA-5	85	0.171	Stable
PUA-10	96	0.095	Stable
PUA-15	98	0.090	Stable
PUA-20	115	0.138	Stable
PUA-25	93	0.126	Stable
PUA-30	77	0.094	Stable
PUA-35	72	0.126	Stable
PUA-40	67	0.240	Stable
PA	59	0.108	Stable

EXPERIMENTAL

Materials

Methyl methacrylate (MMA), butyl acrylate (BA), sodium dodecyl sulfate (SDS), and trimethylamine (TEA) were supplied by Tianjin Guangfu Fine Chemical Research Institute (Tianjin, China). Isophorone diisocyanate (IPDI), 2-hydroxyethyl methacrylate (HEMA), dimethylolpropionic acid (DMPA), dibutyltin dilaurate (DBTDL), and ammonium persulfate (APS) were purchased from Aladdin Chemistry Co. Ltd. (Shanghai, China). All the chemicals above were of analytical grade and used as received. Polyols (DL-2000, DL-400, and MN-400) used in this work were provided by the Polyether Department of SINOPEC Tianjin Pertrochemical Corporation. Their relative molecular masses are 2000, 400, and 400 g/mol, respectively. Their hydroxyl contents are 56, 280, and 410 mg KOH/g, respectively. All the polyols were industrial products and were dehydrated under vacuum at 120°C for 2 h prior to use.

Synthesis of PA Emulsion

The formula of PA emulsion was listed in Table I. A given amount of SDS, APS, distilled water (DW), and 20% of total monomers were dispersed in water in a round-bottom flask which was equipped with a thermometer, a reflux condenser, a mechanical stirrer, and dropping funnels and set up in a water bath for controlling the reaction temperature. The mixture was stirred and heated to 75°C to initiate the polymerization reaction. After 0.5 h, the rest of APS (dissolved in water) and monomers (pre-emulsified with DW and SDS) were dropped gradually into the flask and allowed to react for 2 h at 75°C. Finally, the temperature was risen to 85°C and maintained for another 1 h to achieve complete conversion.

Synthesis of PU Prepolymer

According to Table I, the polymerization reaction was carried out in a four-necked round-bottom flask equipped with a mechanical stirrer under N_2 atmosphere. A certain amount of DL-2000 and DL-400 were added into the reactor and heated to 85°C under stirring. Subsequently, IPDI and DBTDL were fed into the reactor. The temperature was kept at 85°C for 2 h to obtain the NCO-terminated prepolymer. After that, MN-400 (cross-linking agent) and DMPA (carboxylic group donator) were added and the reaction continued for another 3 h.

Preparation of PUA Emulsion

The temperature of PU prepolymer prepared above was cooled to 65°C and TEA was used to neutralize the carboxyl group. After 5 min, the as-prepared PA emulsion was added to PU prepolymer rapidly under vigorous stirring at a speed of 1000 rpm. After 30 min, the PUA composite emulsion (*ca* 30% solid content) was obtained. Then the pH was adjusted to 8∼9 with TEA. PUA emulsions with different mass ratio of PA/PU were got following the same process. In this work, the PUA emulsion was designated as PUA-X. For example, PUA-0 stands for pure PU, and PUA-30 stands for composite PUA containing 30% of PA.

Fabrication of PUA Films

The PUA films were fabricated by pouring emulsions into a Teflon disc and dried under ambient for 24 h. Then the films were peeled off and absolutely dried under vacuum at 50°C. The films (*ca* 0.5 mm thickness) were stored in a vacuum desiccator for further characterization.

Measurements and Characterization

TEM micrographs of the PUA particles were taken using JEM-2100 (JEOL, Japan) with an acceleration voltage of 200 kV. The emulsions were diluted to the appropriate concentration. Samples were stained with 2% phosphotungstic acid solution for 30 s.

The particle size and its distribution of emulsions were analyzed by BI-90 Plus (Brookhaven, USA).

The effect of pH on the stability of PUA emulsion was investigated by a series of solutions with pH values from 1 to 12. The Zeta potentials of the emulsions under different pH were recorded by Nano ZS (Malvern Instruments Ltd., Worcestershire, UK). The dispersive situation of emulsion particles in each pH solution was observed with naked eye.

The FT-IR spectra of the sample films were recorded in the range of 4000–650 cm^{-1} using Nicolet iS5 (Thermo Scientific, USA) at a resolution of 4 cm^{-1}.

Table III. Stability and Zeta Potential of PUA-30 Emulsion under Different pH

pH	Stability	Appearance	Zeta potential (mV)
0.99	Unstable	Serious gel	−1.15[a]
1.98	Unstable	Serious gel	−1.56[a]
2.94	Unstable	Serious gel	−3.58[a]
4.02	Stable	Slight gel	−8.52[a]
6.05	Stable	Clear	−30.32
7.94	Stable	Clear	−43.78
9.10	Stable	Clear	−35.98
9.95	Stable	Clear	−31.23
11.01	Stable	Clear	−47.37
12.03	Unstable	Cloudy	−25.94

[a] The Zeta potential of supernatant was recorded for the unstable samples.

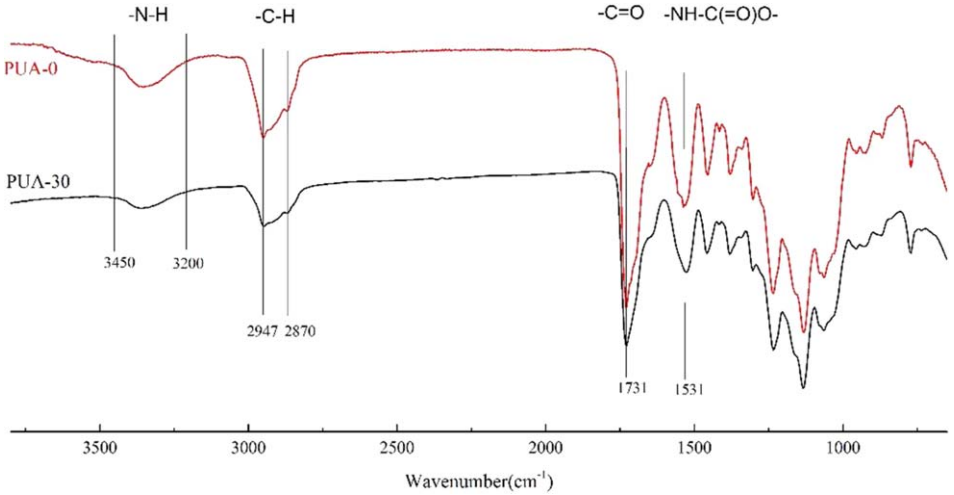

Figure 2. FTIR spectra of PUA-0 and PUA-30 films. [Color figure can be viewed in the online issue, which is available at wileyonlinelibrary.com.]

The surface morphology of PUA film was observed with AFM-5500 (Agilent, USA). Images were acquired in tapping mode using a Nanoprobe cantilever. For AFM measurement, the PUA emulsions were cast onto aluminized paper and dried at 100°C for 2 min.

The water contact angle of the film surface was measured by EasyDrop (FM40, Kruss, Germany) with distilled water.

The water absorption ratio was detected by immersing dried PUA films in distilled water at 25°C. After 48 h, the films were taken out from water and blotted with filter paper to remove the surface water. The water absorption ratio (ω) was calculated as follows[27]:

$$\omega\% = \frac{w_1 - w_0}{w_0} \times 100\% \quad (1)$$

where w_0 and w_1 are the masses of the film before and after absorbing water, respectively.

The hardness values of PUA films were measured using a Shore Durometer A type machine (LX-A, Wenzhou, China) according to ASTM D2240. The values quoted were the average of five readings.

Mechanical properties were collected at room temperature using an Instron Mechanical Tester (ASTM D638). Tensile specimens (35 × 10 × 0.5 mm) were cut from dried films. A cross-head speed of 5 mm/min was used to determine the tensile strength and elongation at break.

The fractured surface morphologies of PUA films were studied by SEM (Hitachi S-4800, Japan) at an accelerating voltage of 5 kV. Samples were scanned with sputtering metal on their surfaces.

TG analysis of PUA films was conducted in an analyzer Perkin-Elmer TGA-7 under a nitrogen flow, at a heating rate of 10°C/min and in the range from 40 to 900°C.

RESULTS AND DISCUSSION

TEM Analysis

TEM micrographs of PUA-0, PA PUA-20, and PUA-30 particles are shown in Figure 1. The pure PU particles were formed by dispersing the PU prepolymer in water. All the particles generated at the same time and were almost with the same evolutionary history. The PU particles were with very small particle size and unimodal particle size distribution. However, the PU particles were very soft; therefore, in the TEM detection, the particles were deformed and the profile of the particles was vague in the image. On the contrary, the pure PA particles (sample PA) were prepared through the classical emulsion polymerization and were stable with emulsifier (SDS). From the formula, we know that the PA polymer is with higher glass transition temperature and the particles are much harder than PU particles. In the TEM detection, the profile of the PA particles remains clearly spherical. The average particle size of PA particles is smaller than 60 nm. While the composite particles were prepared, the PU particles were formed from a flowable state to a particle state in the presence of the PA nanoparticles. So the PA nanoparticles are prone to be encapsulated by PU polymer; therefore, the core–shell structure will be achieved for the PUA composite particles. As in the TEM micrographs, we can see that the particles for PUA-20 and PUA-30 are with clear core–shell structure. The average particle size of the composite particles is about 100 nm. Furthermore, the profile of PUA-30 particles in the TEM micrographs is much clearer than that of PUA-20, as the rigid PA content is higher in PUA-30.

Particle Size Distribution and Storage Stability of PUA Emulsions

The average particle size and its distribution have important effect on properties of PUA emulsions, especially on storage stability and wettability, which decide the commercial value and end use. In Table II are listed the particle sizes and their distributions and stabilities of typical samples. It is obvious that the average particle size initially increases and subsequently decreases as PA content increases. Although the average particle size could be controlled by emulsification condition such as stirring speed and dispersion temperature, it is mainly governed by the concentration of hydrophilic groups and segmented polymeric structure.[28,29] In this work, the effect of different mass ratio (PA/PU) on particle size was investigated. The particle sizes of PUA-0, PUA-5, PUA-20, PUA-30, and PA are 70, 85,

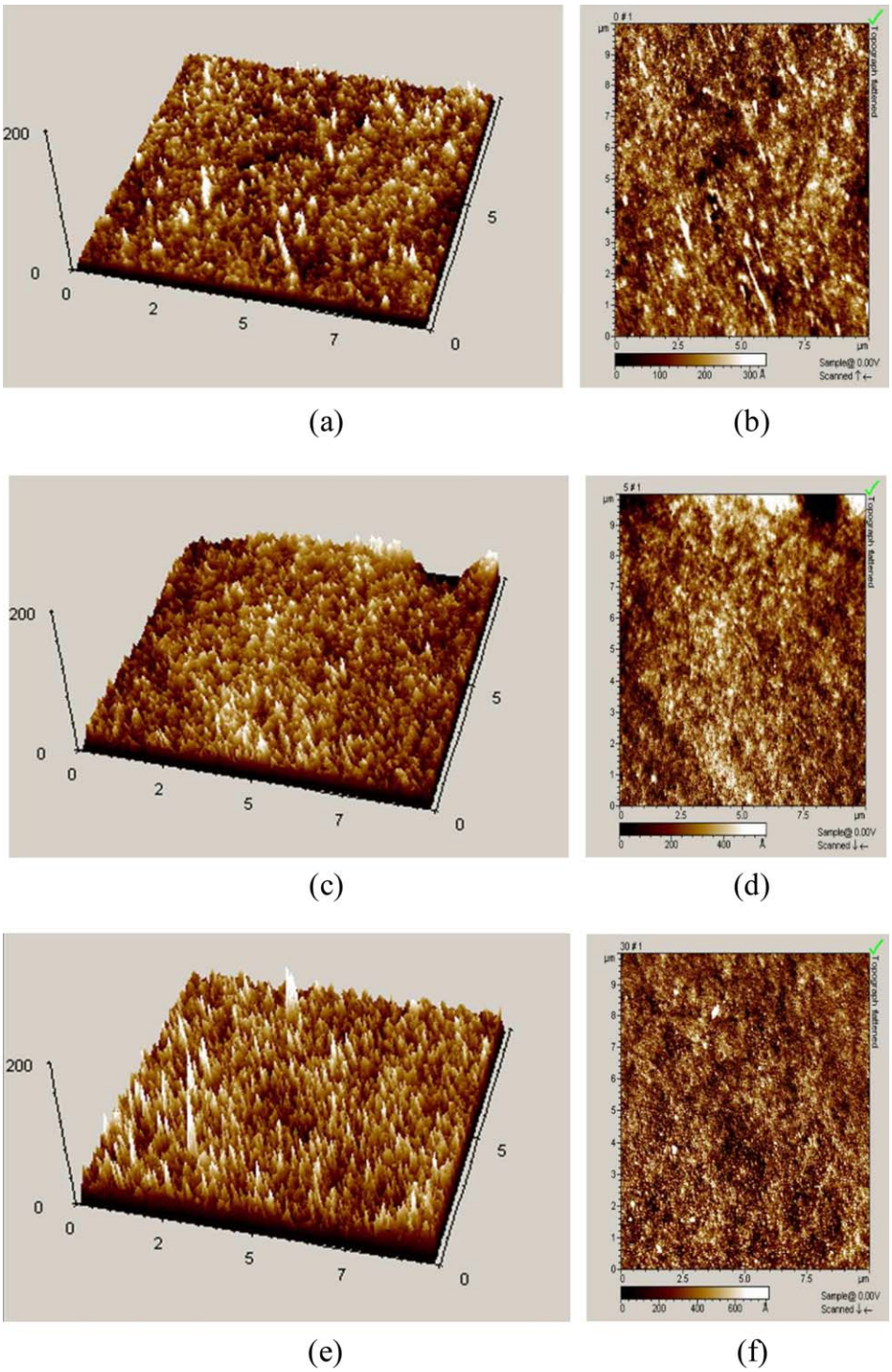

Figure 3. AFM (a, c, and e) 3D height images and (b, d, and f) 2D phase images of PUA-0, PUA-5, and PUA-30 films. [Color figure can be viewed in the online issue, which is available at wileyonlinelibrary.com.]

115, 77, and 59 nm, respectively. The PA emulsion was prepared by classical emulsion polymerization and its average particle size is about 60 nm with unimodal particle distribution. The pure waterborne PU dispersion was prepared with dispersing the PU prepolymer in water and the PU particles were formed with a phase inversion process under vigorous agitation; therefore, the pure PU particles of sample PUA-0 were in nanoscale and with monomodal distribution. Its average particle size is about 70 nm. For the composite PUA emulsions, as the mass ratio of PA/PU varies from 0 to 1/4, the average particle size increases because of the PA particles being encapsulated in PU and formation of the core–shell structured PUA particles. However, as the PA/PU ratio reaches a critical value (*ca* 1/4), the PA particles are too many to be encapsulated in PU shell; therefore, the

Table IV. Water Contact Angle, Average Roughness, and Root Mean Square of PUA Films

Sample no.	Water contact angle (°)	Ra (nm)	RMS (nm)
PUA-0	58.3	3.78	10.70
PUA-5	71.6	4.93	6.54
PUA-10	72.5	—	—
PUA-15	74.7	8.45	11.24
PUA-20	77.4	—	—
PUA-25	78.6	11.51	14.71
PUA-30	83.0	17.44	22.80
PUA-35	82.1	—	—
PUA-40	81.3	—	—

average particle size will become smaller with further increasing the mass ratio of PA to PU because more and more small PA particles will be remained in the composite emulsion without being wrapped in PU shell. In general, the emulsions with particle size being smaller than 200 nm are stable, while with larger sizes (always >1000 nm) are considered to be unstable. From Table II, we can find that the average particle sizes of almost all the emulsion samples are in nanoscale with uniform particle size distribution; therefore, the storage stability of all the samples are longer than 6 months.

Effect of pH on the Stability of PUA Emulsion

The stability of emulsion under different pH plays a key role in practical industry. To study the effect of pH on the stability of PUA emulsion, PUA-30 emulsion was selected and dropped into different pH solution in the range of 1–12. The Zeta potentials and stability of the sample under different pH are shown in Table III. When the pH varies from 6.05 to 11.01, the emulsion remains stable. In general, the stability of PUA emulsion can be controlled by "repulsive force" caused by the same charge between particles. The value of Zeta potential acts as a standard to evaluate the strength of "repulsive force." The larger the absolute value of Zeta potential is, the stronger the "repulsive force" is. Therefore, it means that the more stable the emulsion is. In the pH range of 6.05–11.01, the absolute values of all Zeta potentials are larger than 30 mV. On one hand, as the pH reduces, the stability seriously deteriorates and the emulsion even aggregates. It is obvious that the high hydrogen ion concentration under low pH condition does harm to the emulsion stability which results from anion ions, such as SDS and carboxylate groups.[30] On the other hand, when pH is beyond 12, the emulsion became cloudy, which is possibly caused by the lack of free water due to excess alkaline added.

FTIR Analysis of PUA Films

FTIR spectra of PUA-0 and PUA-30 are displayed in Figure 2. Both FTIR spectra exhibit characteristic peaks of N—H stretching vibration in the range of 3450–3200 cm^{-1} (free and H-bonded —NH). The vibration peaks at 2928 and 2870 cm^{-1} are attributed to the asymmetric and symmetric stretching of aliphatic —CH, respectively. The blending vibration of —NH in —NH—C(=O)O— appears at around 1531 cm^{-1} and the stretching vibration of —C=O in the urethane and acrylates molecules occurs at around 1731 cm^{-1}.[8] Comparing the FTIR spectra of PUA-0 and PUA-30 films, the differences are as follows: (1) the absorbing intensity of —NH and —C=O from PUA-0 is much higher than that of PUA-30; (2) the absorbing width of —NH and —C=O from PUA-0 is also much higher. It is due to that PUA-0 contains more —C=O and —NH groups on the film surface than PUA-30, causing the higher absorbing intensity. Generally, in the FTIR spectra of PA and PU blend, the broader the absorbing peak, the more enhanced the phase mixing.[26] It can be inferred that PUA-0 has slightly higher phase uniformity degree than corresponding to PUA-30. In fact, the FTIR spectra of other samples in the present work show the common trend that the lower the content of PA is, the higher the phase uniformity of the composite PUA films is.

AFM Topography

AFM 3D height images and 2D phase images of typical PUA films (PUA-0, PUA-5, and PUA-30) are shown in Figure 3. The average roughness (Ra) and root mean square (RMS) of the PUA films were calculated and listed in Table IV. Both Ra and RMS become larger with increasing PA content. The results are assigned to the fact that PA particles are more rigid, which causes more phase separation. It may be elucidated that the hydrophobic groups prefer to migrate to the air/polymer interface and occupy the outmost surface in the anneal process, which is responsible for the increment of Ra. The result of AFM is in accordance with the result of water contact angle to be discussed below.

Water Contact Angle and Water Absorption Ratio of PUA Films

The water contact angle is a measurement of the surface wettability. The contact angles of all sample films are summarized in Table IV. We can find that the water contact angles increase from 58.3° to 83.0° with PA content from 0% to 30% in composite PUA. With PA content beyond 30%, the water contact angles almost remain unchanged. Contact angle of a solid film

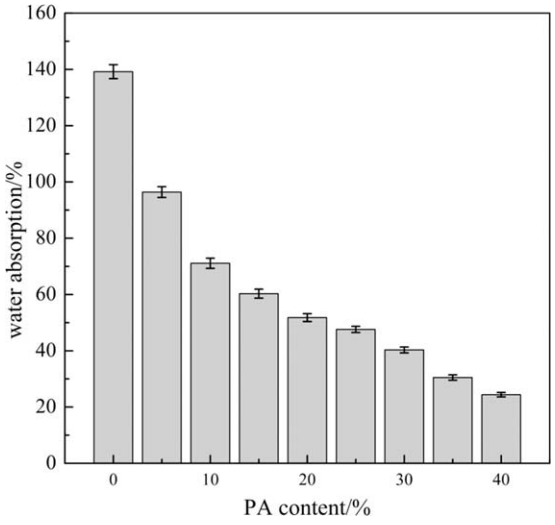

Figure 4. Water absorption ratios of PUA films at different PA content.

Table V. Mechanical Properties of PUA Films

Sample no.	Hardness (Shore A)	Tensile strength (MPa)	Elongation at break (%)
PUA-0	75	7.23	172.28
PUA-5	79	8.62	169.91
PUA-10	82	6.69	153.64
PUA-15	83	5.85	126.82
PUA-20	85	4.68	89.43
PUA-25	89	3.25	56.29
PUA-30	90	3.09	42.65
PUA-35	93	2.34	20.67
PUA-40	95	1.89	10.35

All the values are the average of five readings.

surface relies on chemical composition and surface rough, that is, it increases with hydrophobicity and surface rough.[31] According to Wenzel and Cassie's theory, the surface roughness was one of the most important factors affecting the surface wettability.[32,33] As aforementioned, Ra of composite PUA films varied from 4.93 to 17.44 nm while PA content increased from 5% to 30% (Table IV). In principle, the hydrophobicity will be geometrically enhanced with increase of surface roughness, forming the similar structure to mastoid of the lotus leaves. It may ascribe to more hydrophobic groups with incremented PA loading, which reduces wetting and spreading of water molecules as well as permeability and solubility of gas molecules in PUA films.

The water absorption ratios of different PUA films are illustrated in Figure 4. It should be noted that the water absorption ratio substantially declines from 139.2% to 24.4%. The reinforcing effect is fairly pronounced. Overall improvement in water resistance can be attributed to the incorporation of PA.[34] The type and amount of groups and polymeric network are important factors influencing the water swelling. There exist abundant hydrophilic moieties (—COOH, —COO^-, —NH, and —C═O) in PU molecules, which can form hydrogen bond with water molecules. It can be confirmed by the result of FTIR analysis. As PA is added, PA particles can not only form the hydrophobic polymeric network on the surface, but also weaken the hydrogen bond interaction between hydrophilic groups and water molecules.[35] It can be inferred that PA molecules act as an obstructer that prevents water molecules from penetrating into the inside of PUA films. It is in good agreement with the result of water contact angle.

Hardness and Mechanical Properties

The mechanical properties of PUA films are strongly affected by PA content (Table V). With PA content from 0% to 40%, the tensile strength first increases slightly and then decreases, whereas their elongation at break goes down simultaneously from 172.28% to 10.35%. Meanwhile, Shore A values are observed to monotonically increase from 75 to 95. As reported in literature, the hardness was primarily governed by hard segment content and crystallinity of polymer. The introduction of PA into PU gave PUA films a higher glass transition temperature, resulting in enhanced stiffness of the films.[18] The higher tensile strength was achieved not only by inherent properties of additives (PA in this article), but also by optimizing the dispersion and interface chemistry.[36] When the mass ratio of PA/PU is 1/9, the tensile strength reaches the maximum value of 8.62 MPa. It may be accredited to an effective "forced compatibility" to establish close interaction between PA and PU due to physical cross-linking points. When a tensile is applied to this system, these points can add much fraction and dissipate strain energy.[37] However, higher PA loading leads to serious decrease of the tensile strength, even being lowered to only 1.89 MPa with 10.35% elongation at break, which possibly results from two mainly factors. First, with a further increase in the mass ratio of PA/PU, the compatibility and phase structure between PA and PU become worse.[38] Second, PA contains quantities of PMMA blocks and possesses higher glass transition temperature, leading to more rigid and fragile films. It is in good agreement with the result of the hardness.

Fractured Surface of PUA Films

The dispersion state of PA in PU matrix strongly influences the mechanical property of PUA composite films. Therefore, the dispersion of PA in PU matrix was investigated by observing the fractured surface morphology using SEM. As shown in Figure 5, the fractured surfaces of PUA-0 (pure PU) and PUA-10 films are very flat and there are no wrinkles on the surface, but the morphology of PUA-30 is much more different. It appears fairly

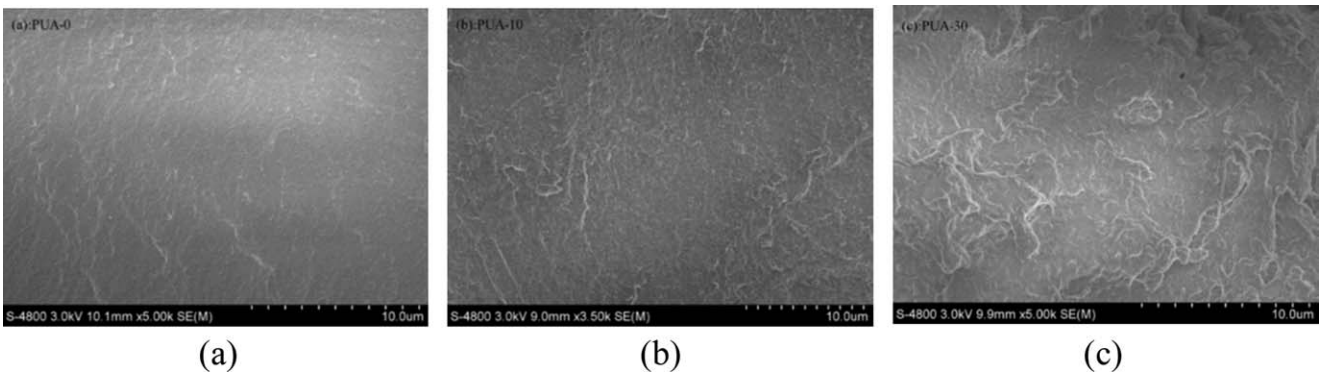

Figure 5. SEM images of fractured surfaces of (a) PUA-0, (b) PUA-10, and (c) PUA-30 films.

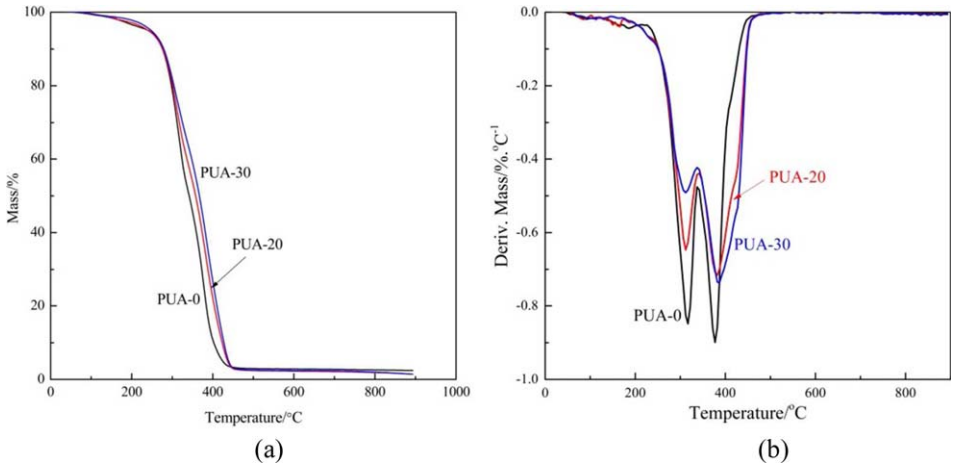

Figure 6. (a) TG and (b) DTG curves of PUA-0, PUA-20, and PUA-30 films. [Color figure can be viewed in the online issue, which is available at wileyonlinelibrary.com.]

rough. There are many irregular projections or aggregations on the surface, resulting from phase separation to some degree. It may be explained as the limited compatibility between PA and PU. So while the addition amount of PA is too much, the tensile strength begins to decrease with respect to PU. The SEM result agrees with that of tensile strength test.

TG Analysis

The thermal behavior of PUA-0, PUA-20, and PUA-30 films analyzed by TG are illustrated in Figure 6. From TG curve, it is found that TG results of PUA-0, PUA-20, and PUA-30 are almost the same. Not only is the outset temperature same (about 250°C), but also the ending temperature (about 450°C) is the same. It can be attributed to the basically same chemical composition, including polyurethane, so they have also same thermal behavior; however, the differences are clear from DTG curve. It can be clearly observed from DTG curve that the degradation of all the samples includes two stages. The first stage from 250 to 350°C is associated to the loss of hard segment of PU and the second stage between 380 and 450°C is corresponding to the later decomposition of soft segment of PU and PA. The result validates the decomposition procedure of typically segmented PU.[6] This again implies that phase separation occurs. Meanwhile, from TG curves we can find that the onset decomposition temperatures of the samples is not very different and subsequently, the residual mass ratios of PUA-20 and PUA-30 are relatively higher than that of PUA-0 at the same temperature, suggesting an improvement of the thermal stability of PUA. The residual mass ratios of PUA-0, PUA-20, and PUA-30 are about 44.51, 52.85, and 58.06%, respectively, when the first stage is over. However, all residual mass ratios are close to 0 after 450°C, indicating that both PA and PU are absolutely degraded. The maximum peaks occur at around 377, 382, and 387°C, respectively. It can be inferred that PA chains with higher bond energy than urethane groups shield and protect PU hard segments from earlier decomposition, and weaken the mass loss ratio.

CONCLUSION

A series of PUA emulsions were prepared by dispersing PU prepolymer in PA emulsion. The effect of the mass ratio of PA/PU on the properties of PUA emulsions and their films were investigated. As PA content augments from 0 to 40%, the average particle size first goes up and subsequently goes down with the maximum particle size of 115 nm while PA content in composite materials is 20%. TEM microscopes show that PUA emulsions consist of PU, PA, and PUA composite particles. The PUA emulsion can remain stable in the range of pH from 6 to 11. The water contact angle continues increasing to the maximum of 83° while the mass ratio of PA/PU reaches 3/7. The average roughness and root mean square of the composite PUA films become larger with increasing PA content. Meanwhile, the water absorption ratios of PUA films decline from about 140 to 24%. The Shore A hardness varies from 75 to 95 and the elongation at break gradually goes down from 172.28 to 10.35%; however, the tensile strength reaches the maximum of 8.62 MPa when the content of PA is 10%. SEM images of the fractured surface of the PUA films also indicate the phase separation of PUA film. In addition, TG analysis result indicates that PUA films have better thermal behavior than that of PU in the range of 250–450°C. Briefly, an alternative way is provided to prepare environmentally friendly WPUA with higher performance for practical applications.

REFERENCES

1. Alexandru, M.; Cazacu, M.; Cristea, M.; Nistor, A.; Grigoras, C.; Simionescu, B. C. *J. Polym. Sci. Part A: Polym. Chem.* **2011**, *49*, 1708.
2. Kim, J. T.; Kim, B. T.; Kim, E. Y.; Park, H. C.; Jeong, H. M. *React. Funct. Polym.* **2014**, *74*, 16.
3. Chen, J. J.; Zhu, C. F.; Deng, H. T.; Qin, Z. N.; Bai, Y. Q. *J. Polym. Res.* **2009**, *16*, 375.
4. Gunes, I. S.; Cao, F.; Jana, S. C. *Polymer* **2008**, *49*, 2223.
5. Madbouly, S. A.; Otaigbe, J. U. *Prog. Polym. Sci.* **2009**, *34*, 1283.

6. Zhang, S. D.; Li, Y. F.; Peng, L. Q.; Li, Q. F.; Chen, S. L.; Hou, K. *Compos. Part A* **2013**, *55*, 94.
7. Bao, L. H.; Lan, Y. J.; Zhang, S. F. *J. Polym. Res.* **2006**, *13*, 507.
8. Sultan, M.; Islam, A.; Gull, N.; Bhatti, H. N.; Safa, Y. *J. Appl. Polym. Sci.* **2015**, *32*, 1.
9. Wu, Z.; Wang, H.; Tian, X.; Xue, M.; Ding, X.; Ye, X.; Cui, Z. *Polymer* **2014**, *55*, 187.
10. Lee, H. T.; Wang, C. C. *J. Polym. Res.* **2005**, *12*, 271.
11. Nam, K. H.; Seo, K.; Seo, J.; Khan, S. B.; Han, H. *Prog. Org. Coat.* **2015**, *85*, 22.
12. Shi, Y. T.; Wu, Y. J.; Zhu, L. Z.; Shentu, B. Q.; Weng, Z. X. *J. Appl. Polym. Sci.* **2015**, *132*, 41266.
13. Cheng, J. Y.; Cao, Y.; Jiang, S. L.; Gao, Y. J.; Nie, J.; Sun, F. *Ind. Eng. Chem. Res.* **2015**, *54*, 5635.
14. Qin, L. L.; He, Y.; Liu, B. H.; Jian, Y; Li, C. J.; Nie, J. *Prog. Org. Coat.* **2013**, *76*, 1594.
15. Wang, X. R.; Shen, Y. D.; Lai, X. J.; Liu, G. J.; Du, Y. *J. Polym. Res.* **2014**, *21*, 367.
16. Zheng, J.; Lu, M. G. *Chem. Pap.* **2015**, *69*, 709.
17. Park, Y. G.; Lee, Y. H.; Rahman, M. M.; Park, C. C.; Kim, H. D. *Colloid Polym. Sci.* **2015**, *293*, 1369.
18. Shin, M. S.; Lee, Y. H.; Rahman, M. M.; Kim, H. D. *Polymer* **2013**, *54*, 4873.
19. Xu, H. P.; Qiu, F. X.; Wang, Y. Y.; Yang, D. Y.; Wu, W. L.; Guo, Q. *Prog. Org. Coat.* **2012**, *73*, 47.
20. Adler, H. J.; Jahny, K.; Vogt-Birnbrich, B. *Prog. Org. Coat.* **2001**, *43*, 251.
21. Jeevananda, T.; Siddaramaiah, G. *Eur. Polym. J.* **2003**, *39*, 569.
22. Spasevska, D.; Daniloska, V.; Leal, G. P.; Blazevska Gilev, J.; Tomovska, R. *RSC Adv.* **2014**, *4*, 24477.
23. Ma, G. Z.; Guan, T. T.; Hou, C. J.; Wu, J. B.; Wang, G.; Ji, X.; Wang, B. J. *J. Coat. Technol. Res.* **2015**, *12*, 505.
24. Athawale, V. D.; Kulkarni, M. A. *Prog. Org. Coat.* **2009**, *65*, 392.
25. Brown, R. A.; Coogan, R. G.; Fortier, D. G.; Reeve, M. S.; Rega, J. D. *Prog. Org. Coat.* **2005**, *52*, 73.
26. Chai, S. L. J. M. M.; Tan, H. M. *Eur. Polym. J.* **2008**, *44*, 3306.
27. Li, M. C.; Ge, X.; Cho, U. R. *Macromol. Res.* **2013**, *21*, 793.
28. Lin, X. F.; Zhang, S. Y.; Qian, J. *J. Coat. Technol. Res.* **2014**, *11*, 319.
29. Li, Y. Y.; Noordover, B. A. J.; Van Benthem, R. A. M.; Koning, C. E. *Eur. Polym. J.* **2104**, *59*, 8.
30. Lee, S. K.; Kim, B. K. *Colloid Interf. Sci.* **2009**, *336*, 208.
31. Lee, T. J.; Kwon, S. H.; Kim, B. K. *Prog. Org. Coat.* **2014**, *77*, 1111.
32. Nakae, H.; Inui, R.; Hirata, Y.; Saito, H. *Acta Mater.* **1998**, *46*, 2313.
33. Cassie, A. B. D. *Discuss. Faraday Soc.* **1948**, *3*, 11.
34. Saeed, A.; Shabir, G. *Prog. Org. Coat.* **2013**, *76*, 1135.
35. Zhang, J. P.; Chen, H.; Wang, A. Q. *Eur. Polym. J.* **2006**, *42*, 101.
36. Pan, H.; Wang, X. D.; Zhang, Y. D.; Yu, L. G.; Zhang, Z. *J. Mater. Res. Bull.* **2014**, *59*, 117.
37. Li, M. C.; Ge, X.; Cho, U. R. *Macromol. Res.* **2013**, *21*, 519.
38. Peng, L. Q.; Zhou, L. C.; Li, Y. F.; Pan, F.; Zhang, S. D. *Compos. Sci. Technol.* **2011**, *71*, 1280.